

# MAGNETISM IN ULTRAFINE Fe AND Co PARTICLES

S. Gangopadhyay<sup>1</sup>, G. C. Hadjipanayis<sup>1</sup>, C. M. Sorensen<sup>2</sup> and K. J. Klabunde<sup>3</sup>

<sup>1</sup>Department of Physics and Astronomy, University of Delaware, Newark, DE 19716.

<sup>2</sup>Department of Physics, <sup>3</sup>Department of Chemistry,  
Kansas State University, Manhattan, KS 66506.

**Abstract** — The magnetic properties of vapor deposited Fe and Co particles in the size range of 50-350 Å have been studied. Magnetization, Mössbauer and structural data show a "core-shell" morphology, where the core is metallic and the shell is a poly-crystalline Fe (Co)-oxide. A sharp reduction in magnetization was observed in particles with a size below 100 Å and this has been attributed to surface/interface spin canting brought about by the ferrite oxide shell. We have systematically studied the effect of various surface chemistries on the hysteretic behavior. The results clearly indicate that the oxide shell controls both the magnitude and the temperature dependence of coercivity.

## 1. INTRODUCTION

For the last several decades the field of nano-scale structures has drawn a great deal of attention [1-6]. Kubo in 1962 [7] dealt for the first time with the effect of finite size on the electronic and various physical properties of small metallic clusters. For instance, he showed that for a 50 Å particle the energy level spacing of quantized electronic states is comparable to  $kT$  at a temperature of 1 K. Thus it is possible to see quantum size effects at finite temperatures. In addition, due to such a large reduction in linear dimension (as compared to the bulk), the boundary or surface conditions play a major role in small particles. Such changes in physical properties brought about by dimensional manipulations can be used to one's advantage. This brings forth the vast applications of fine particles in various fields such as magnetic recording, ceramics, catalysts, medical diagnostics, ferrofluids and pigments in paints [1-6].

Fine particles are routinely used in magnetic recording industry. The conventional recording materials are mostly the acicular and doped  $\gamma$ -Fe<sub>2</sub>O<sub>3</sub>, and CrO<sub>2</sub> particles. A considerable amount of research work has been done to understand the intrinsic and extrinsic properties of these materials. The microstructure and particle morphology have been found to play a major role in determining their magnetic properties. It has been realized that the future needs of the storage industry require particles with much better recording characteristics. That warrants higher remanence (hence higher magnetization), to achieve better signal to noise ratio; higher

coercivity (2-3 kOe) to increase the packing density and to reduce the problem of print-through and accidental erasure. Ultimately to achieve the highest density, smaller but thermally stable particles would be needed. All of these needs could be satisfied by ferromagnetic metallic fine particles.

In this paper we will give an overview of the work that has been done in our lab for the last five years, with a focus on the structural and magnetic properties of Fe and Co particles. The magnetic behavior of Ni fine particles has been published elsewhere [8]. The aim of our work is to investigate systematically the effects of particle size, surface morphology and temperature on the magnetization and coercive behavior of metallic particles. The role of "core-shell" morphology on the reduced magnetization and magnetic hysteresis of small particles will be discussed. The strong temperature dependence of hysteresis brought about by the unidirectional exchange anisotropy will also be discussed. A clear correlation exists between the particle morphology and magnetization of the particles. We have also found a correlation between interparticle interactions and the magnetic properties in these samples.

## 2. EXPERIMENTAL TECHNIQUES

Vapor deposition in an inert gas atmosphere [9] was chosen amongst the various techniques to prepare the fine particles. The details of the method and evaporation specifications can be found elsewhere [10-12]. By this method one could obtain particles with a size in the range of 50 to 350 Å by varying the inert gas pressure from 0.5 to 30 torr. The size of the particles could be easily varied by adjusting the various deposition conditions, such as the inert gas (Ar) pressure, the evaporation source temperature, substrate temperature and the source-substrate distance. The small size of these particles make them chemically very active. Thus a surface "passivation" is imperative. An optimum amount of air/argon (350 mtorr/100 torr) mixture, which resulted in best magnetic properties, was used for passivation.

Three different kinds of particle surface morphologies were prepared. In the first set, particles were passivated by the fore-mentioned air/Ar mixture, resulting in a core-shell morphology consisting of a metallic core surrounded by its oxide shell. In the second set, particles were evaporated onto a Ag coated Kapton substrate, which in turn was again covered with a thin film of Ag in order to protect them from

Manuscript received February 15, 1993. This work was supported by an NSF grant under the grant No. NSF CHE-9013930.

0018-9464/93\$03.00 © 1993 IEEE

oxidation when exposed to atmosphere [11]. Such morphologies will be referred to as  $M/Ag$  sandwiches (where  $M = Fe$  or  $Co$ ). In the third set, the aim was to obtain pure Fe particles with no magnetic surface coating. To achieve this, Fe-Mg particles were obtained by co-evaporating Fe and Mg with the intention to obtain a Mg coating to protect the Fe surface from oxidation. These samples were later heat treated between 200 and 400 °C, resulting in segregation of Fe from an initial Fe-Mg metastable phase.

The particle structure and morphology were characterized by transmission electron microscopy (TEM), and X-ray and selected area electron diffraction (SAD). The magnetic properties were studied using a SQUID magnetometer in the temperature range of 10-300 K and a maximum field of 55 kOe. Mössbauer and X-ray photo-electron spectroscopy (XPS) were also used to investigate the magnetic state and chemical species in the samples.

### 3. MICROSTRUCTURE AND MORPHOLOGY

Particles produced by vapor deposition are chemically very pure and are also free of pores and other morphological irregularities. The size distribution is fairly narrow and resembles a log-normal distribution with  $\sigma$  between 1.1 and 1.4. The smaller particles have a narrower size distribution ( $\pm 10$  Å) as compared to the bigger particles ( $\pm 50$  Å). The shape of the particles obtained in this study is nearly spherical. Deviations from sphericity occur as the particles grow bigger. The maximum aspect ratio is always less than two. Similar morphologies are obtained in the case of Co.

Passivated Fe particles consist of bcc  $\alpha$ -Fe and  $\gamma$ - $Fe_2O_3/Fe_3O_4$  oxides. No evidence of  $\alpha$ - $Fe_2O_3$  has ever been found. Passivated Co consist of fcc-Co with  $CoO/Co_3O_4$  oxides. The diffraction lines due to metal get broader as the particle size decreases whereas the lines due to the oxide phase are always broad. The as-prepared and heat treated Fe-Mg samples contained bcc  $\alpha$ -Fe in addition to Mg and MgO.

### 4. MAGNETIC PROPERTIES

#### 4.1 Magnetization behavior

Fig. 1 shows the change in  $M_s$  with particle size. The maximum value of  $M_s$  obtained was about 90% (of the corresponding bulk value) in the case of Fe and 78% in the case of Co for particles with a size near 300 Å. For particle sizes below 100 Å,  $M_s$  drops very sharply. The reduction in  $M_s$  is expected because of the presence of surface oxides due to passivation; the volume ratio of the oxides to metal gets larger as the particle size decreases. However, much lower  $M_s$  values are observed than those corresponding to  $\gamma$ - $Fe_2O_3$  ( $Fe_3O_4$ ) (average  $M_s$  of  $\gamma$ - $Fe_2O_3$  and  $Fe_3O_4$  is about 90

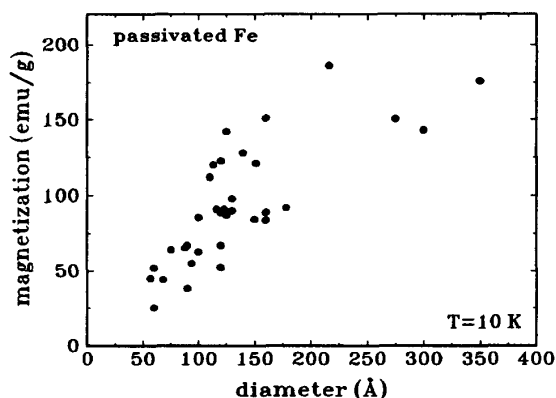


Fig. 1 Variation of saturation magnetization with particle size.

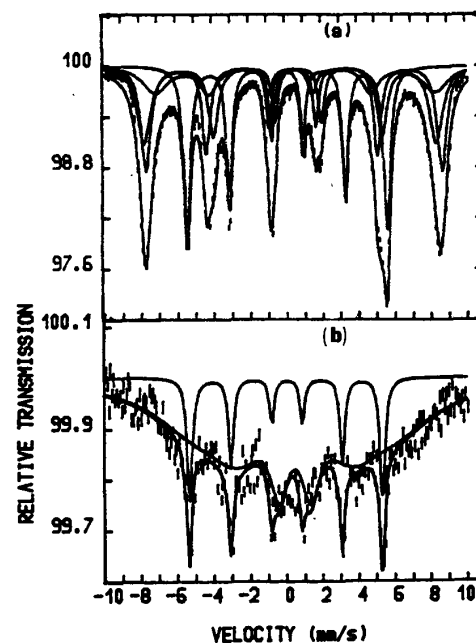


Fig. 2. Mössbauer spectra of passivated 96 Å Fe particles at (a) 4.2 K and (b) 300 K.

Table I. Comparison of saturation magnetization obtained from Mössbauer and SQUID.

Particle Diameter (Å)	Fe wt. %	Fe-oxide wt. %	Magnetization Mössbauer (emu/g)	Magnetization SQUID (emu/g)	% error
275	41.6	58.4	144.6	150	3.6
214	275	72.2	126.6	135	6.22
113	30	70	129.5	120	-7.92
100	16.5	83.5	112	91	-23.08
88	7.3	92.7	100.2	65	-54.15

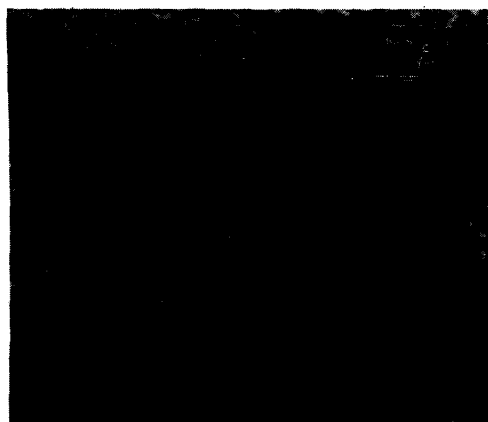


Fig. 3. High resolution TEM of an Fe sample showing a clear "core-shell" morphology, where 'c' or core is of  $\alpha$ -Fe, and 's' or shell is of  $\gamma$ - $\text{Fe}_2\text{O}_3/\text{Fe}_3\text{O}_4$ .

emu/g). Some initial deterioration of the magnetization happens during the first couple of weeks and then  $M_s$  stabilizes to about 70-80% of its initial value [10].

Fig. 2 shows the Mössbauer spectra of 96 Å passivated Fe particles. The 300 K sextet is due to  $\alpha$ -Fe and the broad component which splits at lower temperatures is due to  $\gamma$ - $\text{Fe}_2\text{O}_3$  and/or  $\text{Fe}_3\text{O}_4$ . The presence of the broad doublet in the oxide spectra (instead of a sharp one) indicates interaction between the metallic Fe and the Fe-oxides [13-15]. This feature confirms the presence of oxides around the particles instead of isolated oxide particles. The atomic fraction of the Fe and Fe-oxides obtained from Mössbauer spectra was used to calculate the expected magnetization for the sample and compare it to that obtained from SQUID measurements (Table I). As the particle size decreases below 100 Å, the difference in the experimental and expected  $M_s$  values grows larger, indicating a loss of moment. Using the linear weight ratios and the bulk magnetization of the shell and the core [10] the estimated shell thickness was found to be about 25 Å for Fe and 12 Å for Co. These numbers are consistent with our recent high resolution TEM studies shown in Fig. 3. The core lattice corresponds to Fe (Co) and the polycrystalline shell has a thickness similar to that predicted from the magnetic data.

Reduction in the magnetization with particle size was first observed by Luborsky [16] and Berkowitz [17] in Fe dispersions in mercury and acicular  $\gamma$ - $\text{Fe}_2\text{O}_3$  particles respectively, when the particle size was smaller than 100 Å. They explained the lower values of the moment by considering magnetically dead layers of 1 and 6 Å, respectively. Later studies [18] have clearly shown that the surface layer is not magnetically dead. Coey [19], Morrish [20] and Haneda [21] used Mössbauer studies to propose surface canting brought about by different exchange-coupling at the surface as compared to the core. Recently Pankhurst [22] has proposed

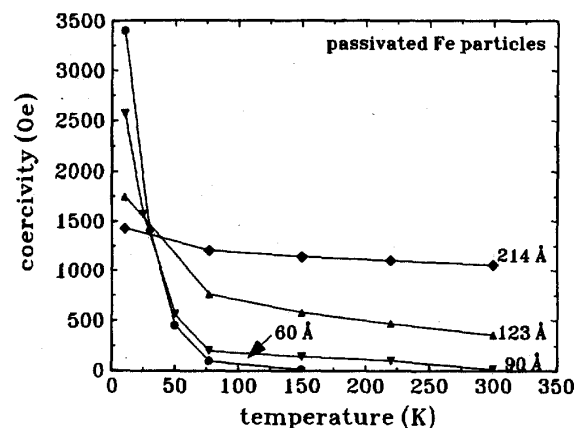


Fig. 4. Temperature and size dependence of coercivity of passivated Fe particles.

that spin canting is an inherent feature of a ferrimagnet and not a finite size effect. Very recently, Parker and Berkowitz [23] have proposed a bulk canting phenomenon to explain the magnetization values deduced from Mössbauer studies of acicular  $\gamma$ - $\text{Fe}_2\text{O}_3$  particles.

Our magnetic, structural and Mössbauer results on small spherical metallic oxide-coated particles (<100 Å) have shown that there is spin canting. The most probable configuration seems to be where the surface/interface spins are canted or pinned. A very recent scanning tunneling microscopy study [24] on magnetite single crystal has shown that the large surface anisotropy caused by  $\text{Fe}^{2+}$  ions is responsible for the surface pinning of moments and hence for the magnetization reduction. Our preliminary data on Mg coated Fe particles show that  $M_s$  is about 200 emu/g, and is independent of particle size (25-400 Å). This may be a very profound result indicating that  $M_s$  does not show finite size effects in pure metallic particles. The reduction in  $M_s$  as observed in various studies has been attributed to the ferrimagnetic species present in the samples.

#### 4.2 Coercivity

**4.2.1 Passivated particles:** Passivated metallic particles show a strong size dependence of  $H_c$ . This was first demonstrated by Kneller and Luborsky [25] in Fe-Co alloy particles. Fig. 4 shows the size and temperature dependence of coercivity in Fe particles. The maximum room temperature coercivity obtained is 1150 Oe (275 Å), and in the case of Co 1500 Oe (350 Å) [26]. Previously,  $H_c$  values of around 1000 Oe have been reported in passivated Fe particles [27]. Particles with a size less than 70 Å diameter are superparamagnetic below room temperature. The size dependence of  $H_c$  is reversed at cryogenic temperatures with the smallest particles having higher  $H_c$ . This can be related to the fact that in

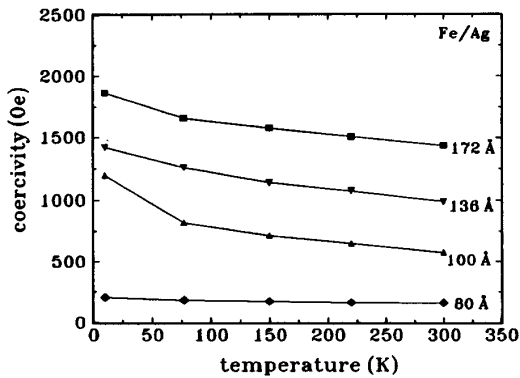


Fig. 5. Temperature and size dependence of coercivity in Fe/Ag particles.

very small particles the surface area and therefore the oxide fraction is large. Similar results were also obtained in the case of passivated Co particles. In the case of Co the temperature dependence of  $H_c$  is more complex at cryogenic temperatures and details have been reported elsewhere [26]. In the next two sections we will illustrate the effect of the reduction of oxide shell thickness on the hysteretic behavior of these particles.

**4.2.2 M/Ag particles:** In the M/Ag series the amount of oxide was minimized (to less than 10 atomic %) and this was confirmed using Mössbauer and XPS studies. Fig. 5 shows the temperature dependence of  $H_c$  for various sizes of Fe/Ag samples. The anomalous behavior observed in the passivated particles (Fig. 4) has now disappeared and at 10 and 300 K the coercivity increases with particle size. The maximum room temperature coercivity in the case of Fe is now 1400 Oe (172 Å) and for Co 1100 Oe (130 Å).

**4.2.3 Fe-Mg particles:** Our preliminary data on co-evaporated Fe-Mg samples did not show any Fe-oxides but only MgO besides  $\alpha$ -Fe and Mg. The particle size was varied from  $\sim 25$  to 400 Å (from X-ray line broadening and TEM) by annealing the Fe-Mg samples at different temperatures (200–450 °C). The coercivity does not change much with temperature and particles with diameter greater than 200 Å are virtually soft,  $H_c \sim 100$  - 300 Oe (at  $T=300$  K). These results are remarkable as they illustrate the crucial role played by the surface chemistry in dictating the entire magnetization behavior of metallic particles. The hysteretic behavior of the particles with the three surface chemistries is compared in Fig. 6.

#### 4.3 Magnetization Reversal

In the past large effort has been devoted to explain the experimentally observed coercivities of metallic particles using

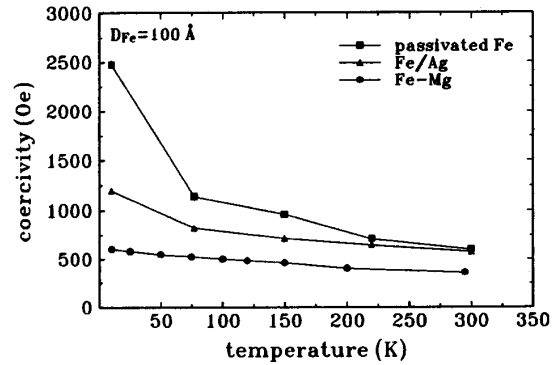


Fig. 6. Temperature dependence of coercivity in Fe particles with different surface morphology. The core size of the passivated Fe sample is 100 Å.

classical as well as dynamical magnetization reversal modes [28–30]. For a better understanding of the correct usage of the various reversal modes, one is referred to a review article by Aharoni [31] and the references therein.

In this article we will only attempt to apply the classical modes of magnetization reversal, such as coherent rotation [32], curling [33–35], buckling [36] and fanning [37] to estimate the coercivity of Fe and Co particles. The reversal modes are dictated by an exchange length scale,  $\lambda_{ex}$  [28,31] (which is below the single domain size). This exchange length depends on material parameters and is given by  $\lambda_{ex} = \sqrt{A/M_s^2}$  where  $A$  is the exchange constant and  $M_s$  the saturation magnetization. For 250 Å passivated Fe and Co particles with  $M_s$  160 and 120 emu/g and  $A = 1 \times 10^{-6}$  erg/cm [38],  $\lambda_{ex}$  is 80 and 94 Å, respectively (if bulk  $M_s$  for Fe and Co are used, the value of  $\lambda_{ex}$  are 57 and 70 Å, respectively). Particles with radius smaller than  $\lambda_{ex}$  would reverse by coherent rotation and the bigger ones by either curling, fanning or buckling [39]. The last two modes are only possible in particles with an aspect ratio greater than those in this study (less than 2). The reduced length scale,  $S$  [29], which is the ratio of particle radius to the exchange length is greater than one, in 250 Å particles of Fe and Co, which implies reversal by curling [39]. Considering only the shape, magnetocrystalline and exchange anisotropy, the nucleation field for curling, for an assembly of randomly oriented single domain particles is given by [32–35]

$$H_N = 0.48 \left[ N_c M_s - 2 \frac{K_1}{M_s} - \frac{2\pi M_s k}{S^2} \right] \quad (1)$$

where  $N_c$  is the demagnetization factor along the polar axis,  $K_1$  the magnetocrystalline constant and  $k$  a function of the aspect ratio of the particle. Using bulk anisotropy constants and the aspect ratios obtained from TEM studies, the estimated coercivities are 200 and 880 Oe for Fe and Co (250 Å), respectively. The coercivity values observed experimen-

tally for Fe and Co particles are much higher (1800 and 2500 Oe (at 10 K), respectively) than those expected by the curling mode (Eqn. 1). These large differences can be attributed to the larger effective anisotropy of the smaller particles and to the core-shell particle morphology which leads to a large exchange anisotropy.

It has been reported repeatedly by various researchers [40,41] that the value of the effective anisotropy constant observed in small particles is much greater than that of the corresponding bulk metal. The anisotropy constant for metallic passivated Fe particles was estimated to be an order of magnitude higher than the bulk [10]. Such large anisotropy can have additional contributions from exchange and surface/interface anisotropy. Also, the effect of inter-/intra-particle interactions can not be ignored. In the next two sections we will discuss briefly the effect of exchange anisotropy and interparticle interactions on the hysteretic behavior of fine particles.

#### 4.4 Exchange anisotropy

Exchange anisotropy was first discovered by Meiklejohn and Bean [42] in compacted Co particles covered by cobaltous oxide. They showed that a unidirectional anisotropy ( $K_u$ ) is induced due to exchange coupling of the interface spins, when two different magnetic species share an interface. When such a system, for instance Co/CoO, is cooled in the presence of a field through the Néel temperature ( $T_N = 295$  K) of the CoO, shifted hysteresis loops are obtained.

Shifted loops were measured in passivated Co particles and the shift was found to be a strong function of particle size [12]. An optimum amount of the surface oxide thickness (or volume) was found to give the maximum shift or  $K_u$  ( $K_u = \text{shift} \times M_s$ ) [41] which was observed in particles with a size near 100 Å. At this size an optimum volume ratio and interface area exist between the ferro- and the antiferromagnetic phases. Below this size some particles get completely oxidized and do not contribute to the exchange coupling, whereas for particles above this diameter the shell thickness is not enough to influence the entire core volume. In reference [12] we have shown that in the case of passivated Co particles, after an optimum amount of shell-thickness is reached, the effect of exchange-coupling is saturated. These results are also predicted theoretically by some recent models discussing the different exchange mechanisms [43,44]. Finite, but small shifts (about 100 to 200 Oe) are also observed in the case of Fe particles.

A very interesting feature of the shift in Co particles is its disappearance at 150 K in all the particles studied and not at about 270 K as observed by Meiklejohn and Bean [41]. This lower temperature is attributed to [12] the superparamagnetism of the polycrystalline Co-oxide shell, which is expected to have a  $T_B$  of 150 K. The reason for the difference

between our data and those of Ref. [41] could be the enhanced interactions among the compacted particles which could lead to an increase in the blocking temperature of the CoO shell [45].

The presence of this exchange coupling which gives rise to an additional anisotropy ( $K_u$ ) in oxide passivated metallic particles, can explain the larger  $H_c$  values and the strong temperature dependence of coercivity. This mechanism becomes even more clear from the hysteretic behavior of  $M/Ag$  and Fe-Mg particles. In  $M/Ag$  particles a very small amount of surface oxide is enough to cause higher coercivity values. Also a smaller thickness in the oxide layer reduces the temperature dependence of coercivity (Figs. 5 and 6). The Fe-Mg data support this scenario further and indicate that in the absence of any surface oxide the particles are magnetically soft and do not exhibit the strong temperature dependence of coercivity.

#### 4.5 Interactions

Interparticle interactions is a many-body problem which is hard to solve, and to date only the systems with a few interacting particles have been studied [46,47]. The particle interactions are mostly the long range dipolar interactions and are routinely studied using remanence curves [48] and dilution experiments [49]. The nucleation field  $H_N$  of Eqn. 1 does not take into account the interactions among particles. But the demagnetizing field of one particle can change the switching field of its neighbors. The presence of canted surface spin structures can complicate the problem of interactions further.

We have studied the interparticle interactions for the passivated metallic particles,  $M/Ag$  particles and Fe-Mg particles and the results have been published in reference [50]. In all the samples the interactions were found to be negative. As the surface oxide-shell thickness decreases, the interactions also decrease. Upon compaction (increased packing) the negative interactions increase, except in the case of very small passivated particles where the interactions actually decrease. This has been attributed to a modified surface spin structure in small particles upon compaction, that would decrease the demagnetizing fields, thus lowering the negative interactions.

#### 4.6 "Core-shell" particle modeling

From the above discussions it is clear that the particle interactions and an exchange term which couples the shell crystallites to core and must be considered in addition to the other energy terms to model the magnetization reversal of the coated small magnetic particles. The oxide shell does not grow epitaxially with respect to the core as seen in Fig. 3. One could minimize the total energy to find the equilibrium angles between the core moment with the various shell

moments. It may be that the easy-axis of the individual oxide crystallites are oriented in a certain crystallographic direction with respect to the core, because the oxide shell grows in the presence of the demagnetization field of the core. The exchange coupling between the two magnetic species (core and shell) is also a function of a length ratio, namely the total diameter to the core diameter. The temperature dependence of the exchange coupling constant (or unidirectional anisotropy) and the superparamagnetism of the oxide shell determine the temperature dependence of the coercivity of the whole particle.

Due to the magnetic non-uniformity of the particles, they will most probably not reverse by a unique reversal mode. In the case of Co particles the shell and core reversals might not occur simultaneously, due to the large difference in their anisotropy constants. Therefore it may be more appropriate to use the dynamic magnetization reversal.

### 5. CONCLUSIONS

Much larger coercivities than those expected from the classical magnetization reversal models have been achieved in passivated Fe and Co particles. The origin of the high coercivity and its temperature dependence is attributed to the surface oxides. It is apparent from the above results that there is a need for an appropriate "dynamical" magnetization reversal model for passivated small spherical particles. The particle morphology and its effect on the magnetic hysteresis behavior is very clear and should not be difficult to incorporate into the existing magnetization reversal models. The explanation of the experimentally observed temperature dependence of coercivity of small particles, by such a theoretical model would be a great achievement.

### ACKNOWLEDGMENTS

We are very thankful to Dr. A. Kostikas at NCSR, "Demokritos", Athens and Dr. V. Papaefthymiou at the University of Ioannina, Greece for their help in acquiring the Mössbauer data.

### REFERENCES

1. E. Matijevic, *Materials Research Bulletin*, pp. 18-20, 1989.
2. E. Matijevic, *Ann. Rev. Materials Sci.*, **15**, p. 483, 1985.
3. M. Ozaki, *Materials Research Bulletin*, pp. 35-40, 1989.
4. R. M. White, *Science*, **229**, p. 11, 1985; Manfred E. Schabes, *J. Magn. Magn. Mat.*, **95**, p. 249 1991.
5. W. P. Halperin, *Rev. Mod. Phys.*, **58**, p. 533 1986.
6. R. D. Shull, R. D. McMichael, L. J. Swartzendruber, and L. H. Bennett, in *Studies of magnetic properties of fine particles and their relevance to materials science*, Edited by J. L. Dormann and D. Fiorani (Elsevier science publisher), p. 161 1992.
7. Ryogo Kubo, *J. Phys. Soc. Jap.*, **17**, p. 975, 1962.
8. S. Gangopadhyay, G. C. Hadjipanayis, C. M. Sorensen and K. J. Klabunde, *Mat. Res. Soc. Symp. Proc.*, **206**, p. 55 1991.
9. C. G. Granqvist and R. A. Buhrman, *J. Appl. Phys.*, **47**, 2200 1976.
10. S. Gangopadhyay, G. C. Hadjipanayis, B. Dale, C. M. Sorensen K. J. Klabunde, V. Papaefthymiou and A. Kostikas, *Phys. Rev. B*, **45**, 9778 1992.
11. S. Gangopadhyay, G. C. Hadjipanayis, S. I. Shah, C. M. Sorensen, K. J. Klabunde, V. Papaefthymiou and A. Kostikas, "Effect of oxide layer on the hysteresis of fine Fe particles", *J. Appl. Phys.*, **70**, p. 5888 1991.
12. S. Gangopadhyay, G. C. Hadjipanayis, C. M. Sorensen and K. J. Klabunde, *J. Appl. Phys.*, **73**, 6964, 1993.
13. K. Haneda and A. H. Morrish, *Surf. Sci.*, **77**, p. 584 1978.
14. I. Tamura, M. Hayashi, *Surf. Sci.*, **146**, p. 501 1984.
15. V. Papaefthymiou, A. Kostikas, A. Simopoulos, D. Niarchos, S. Gangopadhyay, G. C. Hadjipanayis, C. M. Sorensen and K. J. Klabunde, *J. Appl. Phys.*, **67**, p. 4487, May 1990.
16. F. E. Luborsky, *J. Appl. Phys.*, **32**, p. 1715, 1961.
17. A. E. Berkowitz, W. J. Schuele, and P. J. Flanders, *J. Appl. Phys.*, **39**, p. 1261, 1968.
18. J. Lipka, S. Mørup and H. Tøpsøe, *Proceedings of the 3rd International Conference on Soft Magnetic Materials*, Bratislava, p. 763, 1977.
19. J. M. D. Coey, *Phys. Rev. Lett.*, **27**, p. 1140, 1971.
20. K. Haneda and A. H. Morrish, *IEEE Trans. Magn.*, **25**, p. 2597, 1989.
21. A. H. Morrish and K. Haneda, *J. Magn. Mag. Mat.*, **35**, p. 105, 1983.
22. Q. A. Pankhurst and R. J. Pollard, *Phys. Rev. Lett.*, **67**, p. 248, 1991.
23. F. T. Parker and A. E. Berkowitz, *Phys. Rev. B*, **44**, p. 7437, 1991.
24. J. M. D. Coey, I. V. Shvets, R. Wiesendanger and H.-J. Guntherodt, *J. Appl. Phys.*, **73**, p. 6742, 1993.
25. E. F. Kneller and F. E. Luborsky, *J. Appl. Phys.*, **34**, p. 656, 1963.
26. S. Gangopadhyay, G. C. Hadjipanayis, C. M. Sorensen and K. J. Klabunde, *IEEE Trans. Mag.*, **28**, p. 3174, 1992.
27. A. Tasaki, M. Takao, and H. Tokunaga, *Jpn. J. Appl. Phys.*, **13**, p. 271, 1974.
28. Manfred E. Schabes, *J. Magn. Magn. Mat.*, **95**, p. 249 1991.
29. D. Paul and A. Cresswell, submitted to *Phys. Rev. B*.
30. H. Victora, *Phys. Rev. Lett.*, **58**, p. 1788, 1987.
31. A. Aharoni, *IEEE Trans. Magn.*, vol. 22, p. 478, 1987.
32. E. C. Stoner and E. P. Wohlfarth, *Trans. Roy. Soc. London*, **240**, p. 599 1948.
33. W. F. Brown Jr., *Bull. Amer. Soc. Ser. 21*, p. 323 1956.
34. E. H. Frei, S. Shtrikman and D. Treves, *Phys. Rev.*, **106**, p. 446, 1957.
35. A. Aharoni, *J. Appl. Phys.*, **30** Suppl., p. 70S 1959.
36. A. Aharoni, *Phys. Stat. Sol.*, **16**, p. 3, 1966.
37. J. S. Jacobs and C. P. Bean, *Phys. Rev.*, **100**, p. 1060 1955.
38. E. Koester and T. C. Arnoldussen, in: *Magnetic Recording*, vol. 1, eds. C. D. Mee and E. D. Daniel, p. 99, McGraw-Hill, New York, 1987.
39. W. F. Brown Jr., *Magnetostatic Principles in Ferromagnetism*, p. 202, Amsterdam: North Holland, 1962.
40. G. Xiao and C. L. Chein, *J. Appl. Phys.*, **57**, p. 1280, 1987.
41. W. H. Meiklejohn and C. P. Bean, *Phys. Rev.*, **105**, p. 904, 1957.
42. W. H. Meiklejohn and C. P. Bean, *Phys. Rev.*, **102**, p. 1413 1956.
43. A. P. Malozemoff, *J. Appl. Phys.*, **63**, p. 3874 1988.
44. D. Mauri, H. C. Siegmann, P. S. Bagus and E. Kay, *J. Appl. Phys.*, **62**, p. 3047, 1987.
45. S. Mørup, M. B. Madsen, J. Franck, J. Villadsen and C. J. W. Koch, *J. Magn. Magn. Mat.*, **40**, p. 163, 1983.
46. H. N. Bertram, *IEEE Trans. magn.*, vol. 22, p. 466, 1986.
47. Y. D. Yan, E. Della Torre, *J. Appl. Phys.*, **67**, p. 5370, 1990.
48. K. O'Grady, *IEEE Trans. magn.*, vol. 26, p. 1870, 1990.
49. J. E. Knowles, *IEEE Trans. magn.*, vol. 21, 2576, 1985.
50. S. Gangopadhyay, G. C. Hadjipanayis, C. M. Sorensen and K. J. Klabunde, to appear in the same issue of *IEEE Trans. magn.*, Sept. 1993 (same issue).